Theoretical study of substitutional group IV impurities in InP

P K Khowash

Department of Physics, West Virginia University, Morgantown, WV 26506, USA

Abstract. The electronic structure of group IV impurities in InP has been analysed using a discrete variational X_α self-consistent field method in the embedded scheme within the local-density framework. The pure semiconductor gap is calculated to be 1.44 eV in very good agreement with the experimental value of 1.41 eV. The defected clusters are studied by substituting C, Si, Ge and Sn at the central In site. All the impurities but C show a donor-like behaviour with states introduced deep in the gap region of the host semiconductor. The charge distributions and the density of states are calculated. Comparison with experimental results are made wherever available.

1. Introduction

The electrical properties of impurity-doped semiconductors has drawn much attention in the recent years, for its scientific interest and industrial applicability. Among the III–V semiconductors, InP is particularly interesting owing to its higher mobility than other semiconductors such as Si or GaAs, and a high peak-to-valley ratio in the velocity-electric field characteristics, which are of great importance for high-speed devices. The group IV elements as impurities in III–V compound semiconductors are of special interest as they can substitute on either the cation or the anion site. These impurities (otherwise called amphoteric dopants) can behave either as a donor by substituting on the In site, or as an acceptor when occupying the P site. In practice, carbon enters as a residual impurity in InP when vitreous carbon boats are used for growing crystals by liquid-phase epitaxial layers method (Dean *et al* 1979), while silicon has an abrupt doping profile because of its minimum surface segregation during crystal growth which makes the silicon impurity well suited to fabrication of microwave and opto-electronic devices (Cho 1975). Ge doping at about 10^{19} cm^{-3} in InP is utilised to produce dislocation-free material (Brown *et al* 1981) whereas doping with tin has been used as a substrate for device fabrication. Heavy doping of Sn in InP (Schwabe *et al* 1986) also shows gap shrinkage representing the self-energy of the interacting carriers that affect the characteristics and performance of laser devices. However, these results are difficult to analyse if no accurate detailed energy level structure is available. This motivated us to use a discrete variational (DV) X_α self-consistent field method (Ellis and Painter 1970) to study the charge distribution, the defect levels within the gap region of the host semiconductor (obtained from the self-consistent one-electron energy spectra) and the density of states for C, Si, Ge and Sn as substitutional impurities in InP at the In site.

2. Method

The ground-state electronic structures of the ideal and defected clusters extracted from the solid are obtained self-consistently using the DV–linear combination of atomic orbitals (LCAO) method in the embedded scheme within the local-density theory (Ellis 1968, Ellis *et al* 1977; Baerends *et al* 1973, Ellis and Painter 1970). A microcrystal extending out to 17–20 au from the centre of the cluster and consisting of 250–300 atoms is generated around the atoms in the cluster to simulate the solid. The main idea is to suppress surface or cluster size effects by making the peripheral atoms sense a potential similar to that found in the bulk crystal.

The non-relativistic one-electron Hamiltonian in the Hartree–Fock–Slater (HFS) model (Slater 1974, Ellis *et al* 1977) of the self-consistent one-electron local-density formalism is written (in Hartree units) as

$$H(r) = -\tfrac{1}{2}\nabla^2 + \int \frac{\rho(r)}{(r-r')}\,\mathrm{d}r' - \sum_\nu \frac{Z_\nu}{(r-R_\nu)} + V_{\mathrm{ex}}. \tag{1}$$

The second and the third terms on the right-hand side constitute the electronic and nuclear contributions, while the truly non-local Hartree–Fock exchange–correlation is approximated by the X_α potential, dependent only on the local charge density:

$$V_{\mathrm{ex}} = -(3\alpha/\pi)[(3\pi^2/4)\rho(r)]^{1/3} \tag{2}$$

for α varying between $\tfrac{2}{3}$ and 1.

Molecular orbital eigenfunctions $\psi_i^\beta(r)$ for the one-electron Hamiltonian stated above are expanded in terms of a basis set of symmetry orbitals $\varphi_j^\beta(r)$:

$$\psi_i^\beta(r) = \sum_j \varphi_j^\beta(r)C_{ji}^\beta. \tag{3}$$

Here $\beta = (k, \lambda)$ and the φ are chosen to be those LCAO molecular orbitals centred on the different cluster atom sites that transform as the λth row of the kth irreducible representation of the cluster point group.

Then the standard condition that the expectation value of the operator $H - \varepsilon$ be stationary with respect to variations in C_{ji}^β leads to a set of Rayleigh–Ritz type of secular equations compactly written as

$$(H - \varepsilon\mathbf{S})C = 0. \tag{4}$$

In the DV method (Ellis 1968), the Hamiltonian H and the overlap matrix $\mathbf{S}$ are evaluated as weighted sums over a set of sampling points r_k with weight functions $W(r_k)$:

$$H_{ij} = \sum_k W(r_k)\varphi_i^{\beta*}(r_k)H\varphi_j^\beta(r_k) \tag{5}$$

and

$$S_{ij} = \sum_k W(r_k)\varphi_i^{\beta*}(r_k)\varphi_j^\beta(r_k). \tag{6}$$

The molecular orbital eigenfunctions and eigenvalues are obtained as a solution of equation (4). The lowest-energy molecular orbitals are filled successively with cluster electrons up to a self-consistently obtained Fermi energy using Fermi–Dirac statistics. The variational basis functions assigned to In and P are [Pd]$5s^25p^1$ and [Ne]$3s^23p^3$ while those due to C, Si, Ge and Sn are [He]$2s^22p^2$, [Ne]$3s^23p^2$, [(Ar)3d]$4s^24p^2$ and [Pd]$5s^25p^2$.

These are generated by numerical atomic procedures. On the first self-consistent iteration a certain number of electrons is allocated to the cluster and the occupation numbers of the atomic orbitals are specified. This yields a cluster and crystal charge density which is merely the sum of the spherically symmetric charges centred on each atom. The Coulomb potential for each spherically symmetric distribution is given by the one-dimensional integral

$$V(r) = 4\pi \left(\frac{1}{r} \int_0^r \rho(r')r'^2 \, \mathrm{d}r' + \int_r^\infty \frac{\rho(r')}{r'} r'^2 \, \mathrm{d}r' \right) - \frac{Z_i}{r} \tag{7}$$

and the total non-spherical potential is just the sum of each of the spherically symmetric contributions from all the atoms in the microcrystal, conveniently written as an Ewald-type summation (Tosi 1964) with two rapidly convergent series. Electrons in the cluster sampling the potential wells of the atoms exterior to the cluster tend to lower the energy of the valence orbitals as they try to occupy these wells. In practice, the cluster wavefunctions must remain orthogonal to the occupied exterior atoms and this effect is simulated by truncating the attractive potential wells around the exterior nuclei at some radius R_w to some value V_w typically chosen about the Fermi energy.

Finally the total density of states is given by

$$D(E) = \sum_p \frac{\gamma g_p / \pi}{(\varepsilon - \varepsilon_p)^2 + \gamma^2} \tag{8}$$

where g_p is the degeneracy of the level ε_p for the pth molecular orbital. The value of the Lorentzian parameter γ is chosen to be 0.4 eV to obtain a continuous density of states derived from the discrete cluster eigenstates.

3. Results and discussion

A 17-atom cluster consisting of a central In atom, 4 neighbouring P atoms and 12 distant In atoms is scooped out of the solid to form our ideal host. The atoms in the cluster InP_4In_{12} are in a tetrahedral configuration; hence the energy levels are designated according to the irreducible representation of the tetrahedral point group. The defected clusters InP_4In_{12} are then studied by substituting the impurities at the central In site.

The integrated volume charges and the Mulliken population analysis for the pure semiconductor InP cluster are shown in table 1, second column. The volume charges are obtained by integrating over the atomic Wigner–Seitz volumes. The calculated ionicities of In and P differ slightly owing to their size effects and the non-stoichiometry of the cluster chosen. A band gap of 1.44 eV is obtained from the self-consistent one-electron energy spectra in good agreement with the experimental value of 1.41 eV. The band gap increases by 0.1 eV when a transition-state calculation is performed.

The cluster eigenvalues obtained self-consistently are now broadened with a Lorentzian of constant width 0.4 eV, to simulate a continuous density of states. The total density of states for the host semiconductor is shown in figure 1. The P 3s states lie deep in the valence band, while the In 5s levels show up at 4.4 eV above the P 3s peak. Adjacent to the In 5s peak is a smaller peak of mostly In 5s (68%) character along with some contributions from P 3s and In 5p. The peak just below the Fermi level is composed of 45% of P 3p and 41% of In 5p functions along with a 14% contribution from P 3s and 1% from In 5s character. The large peak just above the Fermi level is mainly due to

Table 1. Integrated volume charges and the Mulliken population analysis for the pure semiconductor InP and C, Si, Ge and Sn as substitutional impurities in InP, at the In site.

	InP	InP:C	InP:Si	InP:Ge	InP:Sn
			Volume charge (integration over atomic Wigner–Seitz cell)		
In	48.83	48.58	48.62	48.62	48.65
P	15.30	15.33	15.41	15.42	15.47
Impurity		6.58	13.72	31.70	49.13
			Mulliken population analysis		
In 5s	1.83	1.90	1.90	1.89	1.89
In 5p	0.82	0.72	0.77	0.78	0.81
Net charge	0.35	0.38	0.33	0.33	0.30
P 3s	1.79	1.83	1.80	1.80	1.78
P 3p	3.61	3.47	3.52	3.52	3.56
Net charge	−0.40	−0.30	−0.32	−0.32	−0.34
		C 2s 1.88	Si 3s 1.70	Ge 4s 1.75	Sn 5s 1.55
		C 2p 2.45	Si 3p 1.97	Ge 4p 1.92	Sn 5p 1.66
	Net charge	−0.33	0.33	0.33	0.78
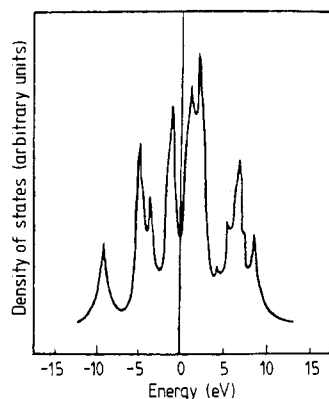
Figure 1. Total density of states for the pure semiconductor InP.

In 5p. The In 5p character starts to build up at about −3.4 eV until it reaches a maximum at 2.7 eV and then decreases. The multiple humps in the conduction band are hybridised P 3p and In 5p functions with a small admixture of In 5s functions. The Fermi level in our calculation is pinned at the last filled or partially filled state.

The Mulliken population for C occupying the In site in InP is shown in table 1, third column. The impurity picks up 0.33 electrons, indicating the dopant to be an acceptor. In regard to the electron count, C with four valence electrons is expected to be a donor when substituted at the In site, thereby removing three valence electrons. Our calculations are in contradiction with donor-like behaviour seen in vapour-phase epitaxial GaAs (Reynolds *et al* 1982). On the other hand, the emission bands in the photoluminescence experiments (Donnelly and Hurwitz 1977, Vaidyanathan 1981) suggest acceptor-like behaviour in other semiconductors owing to the same carbon impurity. Again, similar experiments (Reynolds *et al* 1982) reveal donor-like states ascribed to C in GaAs, at the Ga site, called the X_3 centre.
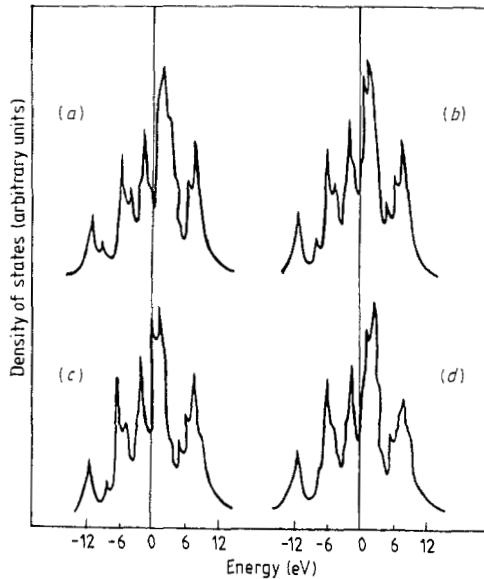
Figure 2. Total densities of states: (*a*), InP:C; (*b*), InP:Si; (*c*), InP:Ge; (*d*), InP:Sn.

When carbon is substituted at the In site, it introduces a level of t_2 character, composed of 45% C 2p, 45% In 5p, 8% P 3p and 2% P 3s, in the band-gap region at $E_v + 0.41$ eV. Experimentally both shallow and deep levels are detected (Pantelides 1975, Donnelly and Hurwitz 1977, Skromme *et al* 1984, Reynolds *et al* 1982). The deep-level transient spectroscopy measurements by Sun (1986) identifies levels at $E_v + 0.4$ eV and $E_c - 0.45$ eV, respectively. Carbon-related deep levels are also detected in other III–V semiconductors such as GaP (Scheffler *et al* 1981) and GaAs (Scolfaro *et al* 1986). The application of an empirical Koster–Slater model (Hjalmarson *et al* 1980) to C at the Ga site in GaAs within the orthogonalised tight-binding framework leads to a state in the gap region at $E_c - 1.0$ eV. The use of a self-consistent pseudo-function method (Scheffler *et al* 1981), on the other hand, predicts the state to be at $E_c - 1.3$ eV for C in GaP.

The total density of states for C-doped InP is shown in figure 2(*a*). The P 3s peak forms the bottom of the valence band. The small peak peeping out next to P 3s peak can be attributed to C 2s and is composed of 53% C 2s, 26% P 3s, 7% P 3p, 13% In 5s and 1% In 5p. The In 5s and P 3p bands differ by approximately 4.9 eV. The peak just below the Fermi energy consists of 45% P 3p, 14% In 5s and 41% In 5p. The C 2p state tends to show up between the P 3p and In 5s states at about 3.0 eV below the Fermi energy.

We now replace the central carbon atom by silicon. Silicon is known to be a donor in InP (Holmes and Kamath 1981). However, acceptor levels have also been identified (Pomrenke 1983) in vapour-phase epitaxial InP implanted in silicon. The aging effect at room temperature increases the mobility of silicon-doped InP but at the same time decreases the carrier concentration (Roth *et al* 1982). Our calculations identify the silicon impurity to be a donor when substituted at the In site in agreement with Fourier transform photoionisation (Cook *et al* 1982), magnetophotoluminescence (Dean *et al* 1984) and far-infrared laser magneto-optical (Armistead *et al* 1984) spectroscopy experiments where the species are tentatively identified as donor in undoped and intentionally doped

InP. The amount of charge given out is exactly equal to the charge drawn into C 2s and 2p state. The neighbouring P and In atoms becomes less ionic compared with the ideal host semiconductor.

The self-consistent one-electron energy spectra for InP : Si shows a trap level of a_1 character composed of 3% Si 3s, 42% P 3p and 52% In 5p in the gap region, at 0.99 eV above the valence band edge. This is in very good agreement with the deep-level transient spectroscopy measurements (Sun 1986) where a level at 0.32 eV below the conduction band edge (i.e. at 0.99 eV above the valence band edge) is detected. Theoretically (Vogl 1981, Koster and Slater 1954), Si on the In site was predicted to have an ionisation energy of $E_c - 0.1$ eV. In our calculations, the $6t_2$ level which was formally in the gap at $E_v + 0.41$ eV for carbon is now found at 0.25 eV above the conduction band edge.

The total density of states for a silicon impurity in InP at the In site (figure 2(b)) shows a similar overall structure as in carbon-doped material except for the fact that the Si 3s and 3p states move closer to the In 5s peak and a new peak appears in the valley above the Fermi level. The difference in energy between the Si 3s and In 5s peaks is almost half the value of the difference between the C 2s and In 5s peaks. The peak at 4 eV below the Fermi energy is composed of 13% Si 3p, 9% P 3s, 16% P 3p, 59% In 5s and 3% In 5p. Again the shallow peak in the valley at about 4.8 eV, in the conduction band, is mainly due to 28% Si 3p, 7% P 3s, 18% P 3p, 2% In 5s and 45% In 5p. The Si states, therefore, are hybridised appreciably with host s and p states and become delocalised.

Germanium is a minor contaminant in InP. It may be noted here that the group IV elements are known to substitute in either the group III (In) or the group V(P) site in III–V (InP) semiconductors, converting them to either n-type and p-type materials. As stated earlier, the occupancy of these impurities at the cation site leads to a donor-like behaviour owing to the presence of an extra electron while the occupancy at the anion site leads to an acceptor-like behaviour because there is one less electron, resulting in an amphoteric character. However, only n-type materials are reported in Ge-doped InP (Whelan *et al* 1960). Annealing of p-type germanium-doped GaAs at a high As pressure resulted in n-type GaAs (McCaldin and Harada 1960), but Si and Ge have a greater probability of substituting in the In site rather than the P site in InP because of size effects. As carbon has a smaller radius than both In and P, it can substitute at either site. Preliminary calculations indicate that C prefers to occupy the P site in InP (Khowash and Ellis 1990). So only donor-like states are expected for Si- and Ge-doped InP. Our calculated results identify the Ge impurity to be a donor (see Table 1, fifth column). It is interesting to note that the charge distribution remains unaltered while substituting Si with Ge.

The germanium impurity introduces a level of a_1 character in the gap region of the host semiconductor. This level contains one electron from the impurity and is placed at 0.92 eV above the valence band edge (i.e. $E_c - 0.54$ eV). Other theoretical calculations (Vogl 1981) predict a level at $E_c - 0.2$ eV in contrast to the experimental (Sun 1986) value of $E_v + 0.25$ eV. Ge at the In site has also been identified as a donor with a binding energy of 5.76 meV (Skolnick *et al* 1984a). Steady-state photocapacitance experiments performed at 77 K detect both shallow- and deep-gap levels, but most of these levels are assigned to defect complexes such as Ge_PS_{In}, $Ge_{In}V_P$ and $Ge_{In}Ge_P$, where V_P denotes a vacancy at the P site.

The density of states for the germanium impurity at the In site is shown in figure 2(c). While the P 3s state is again at the bottom of the conduction band, the In 5s is now approximately 4.8 eV above the P 3s band. The Ge 4s (49% Ge 4s, 17% P 3s, 14% P 3p,

19% In 5s and 1% In 5p) states lie close to the In 5s states but now stands out at about -7.1 eV. No major difference in the density of states is noticed because the atomic energies of Si 3s and 3p states are very close to the 4s and 4p states of germanium. The small peak at 5.2 eV above the Fermi level is made up of 27% Ge 4p, 6% P 3s, 15% P 3p, 3% In 5s and 49% In 5p functions. The multiple peaks above the Fermi level are due to strong hybridisation of P 3p, In 5p and Ge 4p functions.

Recent experimental studies (Brozel *et al* 1984) show that almost 100% of the tin atoms occupy In lattice sites. S seems to be an unavoidable contaminant with ionisation energy close to that of Sn (Skolnick *et al* 1984b; Lee *et al* 1987). We show the integrated volume charges and the Mulliken population analysis for InP : Sn in table 1, sixth column. Our calculated results indicate that Sn is a donor with a net charge of nearly three quarters of an electron. The ionicity of neighbouring P increases whereas the distant In becomes atomic like compared with the ideal host and other group IV elements considered so far. Sn, when introduced at the central In site, introduces a level of a_1 character, with one electron, close to the conduction band edge at $E_c - 0.19$ eV. This level has contributions from Sn 5s (6%), P 3s (2%), P 3p (3%), In 5s (2%) and In 5p (87%). The t_2 level, formally in the band-gap region for carbon, now forms the first empty state in the conduction band at $E_c + 0.22$ eV.

The total density of states for Sn-doped InP is shown in figure 2(*d*). The P 3s state is, as usual, located deep in the valence band. Unlike other group IV elements, the impurity s state nearly merges with the In 5s state. The largest contribution of the Sn 5s state is 45% at about -6.0 eV. The peaks around the Fermi energy (just below and above) are hybridised s–p states (48% P 3p, 10% In 5s and 42% In 5p) and nearly pure In 5p (6% Sn 5p and 94% In 5p) functions. The state at 5.3 eV above the Fermi energy is composed of 24% Sn 5p, 2% P 3s, 5% P 3p, 5% In 5s and 64% In 5p functions.

In conclusion, we have performed a fully self-consistent electronic structure calculation using a DV method in an embedded scheme within the local-density formalism to study the electronic structure, the charge distribution, the detection of impurity levels in the gap region of the host semiconductor and the density of states for the group IV elements as impurities in InP, at the In site. For the pure semiconductor a band gap of 1.44 eV is calculated, in good agreement with optical measurements. The impurities are substituted at the central In site one after another to study the defected clusters, thereby maintaining the cluster symmetry. All the group IV elements but carbon doped in InP are found to be donors, in agreement with the electrical characteristic data of InP implanted with group IV elements. Deep-trap levels for C, Si, Ge and Sn are observed at 0.41 eV, 0.99 eV, 0.92 eV and 1.25 eV, respectively, above the valence band edge. The substitution of any impurity at the central indium site, in general, will cause a local lattice contraction or expansion depending on the nature of impurity introduced, thereby reducing the crystal symmetry. No lattice relaxation whatsoever was accounted for in our calculations. We propose to undertake these effects in future. Our calculated results for the frozen lattice are in fair agreement with optical experiments where deep levels are reported for these group IV impurities.

References

Armistead C J, Knowles P, Najda S P and Stradling R A 1984 *J. Phys. C: Solid State Phys.* **17** 6415
Baerends E J, Ellis D E and Ros P 1973 *Chem. Phys.* **2** 41
Brown G T, Cockayne B and MacEwan W R 1981 *J. Cryst. Growth* **51** 369

Brozel M R, Foulks E J, Grant I R, Li L, Hurle D T J and Ware R M 1984 *Proc. 6th Int. Conf. Vapour Growth and Epitaxy and 6th Am. Conf. on Crystal Growth (Atlantic City, NJ), 15–20 July 1984* (Amsterdam: North Holland)

Cho A Y 1975 *J. Appl. Phys.* **46** 1733

Cook L W, Tashima M M, Tabatabaic N, Low T S and Stillman G E 1982 *J. Cryst. Growth* **56** 475

Dean P J, Robbins D J and Bishop S G 1979 *J. Phys. C: Solid State Phys.* **12** 5567

Dean P J, Skolnick M S and Taylor L L 1984 *J. Appl. Phys.* **55** 957

Donnelly J P and Hurwitz C E 1977 *Appl. Phys. Lett.* **31** 418

Ellis D E 1968 *Int. J. Quantum Chem.* **2** 535

Ellis D E, Banesh G A and Byrom E 1977 *Phys. Rev.* B **16** 3308

Ellis D E and Painter G S 1970 *Phys. Rev.* B **2** 2887

Hjalmarson H P, Vogl P, Wolford D J and Dow J D 1980 *Phys. Rev. Lett.* **44** 810

Holmes D E and Kamath G S 1981 *J. Cryst. Growth* **54** 51

Khowash P K and Ellis D E 1990 *Phys. Rev.* to be submitted

Koster and Slater J C 1954 *Phys. Rev.* **95** 1167

Lee B, Pan N, Stillman G E and Hess K L 1987 *J. Appl. Phys.* **62** 1129

McCaldin J O and Harada R 1960 *J. Appl. Phys.* **31** 2065

Pantelides S T 1975 *Festkörperprobleme (Advances in Solid State Physics)* vol XV ed. J Treusch (Braunschweig: Vieweg) p 149

Pomrenko G S 1983 *J. Cryst. Growth* **64** 158

Reynolds D C, Litton C W, Smith E B, Yu P W and Bajaj K K 1982 *Solid State Commun.* **42** 827

Roth T J, Skromme B J, Low T S and Stillman G E 1982 *Semiconductor Growth Technology* ed. E Krikorian (Bellingham, WA: ISOE) p 36

Scheffler M, Pantelides S T, Lipari N O and Bernholc J 1981 *Phys. Rev. Lett.* **47** 413

Schwabe R, Haufe A, Gottschalch V and Unger K 1986 *Solid State Commun.* **58** 485

Scolfaro L M R, Pintanel R, Gomes V M S, Leite J R and Chaves A S 1986 *Phys. Rev.* B **34** 7134

Skolnick M S, Dean P J, Taylor L L and Anderson D A, Najda S P, Armistead C J and Stradling R A 1984a *Appl. Phys. Lett.* **44** 881

Skolnick M S, Dean P J, Groves S H and Euphal E 1984b *Appl. Phys. Lett.* **45** 962

Skromme B J, Stillman G E, Oberstar J D and Chan S S 1984 *Appl. Phys. Lett.* **44** 319

Slater J C 1974 *The Self Consistent Field for Molecules and Solids* (New York: McGraw-Hill)

Sun Shih Wei 1986 *PhD Thesis* Northwestern University

Tosi M P 1964 *Solid State Phys.* **16** 1 (New York: Academic)

Vaidyanathan K V 1981 *Gallium Arsenide and Related Compounds (Oiso) 1981* ed. T Sugano (Inst. Phys. Conf. Ser. 63) p 395

Vogl P 1981 *Festkörperprobleme (Advances in Solid State Physics)* vol XXI ed. J Treusch (Braunschweig: Vieweg) p 191

Whelan J M, Struthers J D and Ditzenberger J A 1960 *Properties of Elemental and Compound Semiconductors* ed. H C Gatos (New York: Interscience) p 141